Performance of anode-supported solid oxide fuel cell with La$_{0.85}$Sr$_{0.15}$MnO$_3$ cathode modified by sol–gel coating technique

Sung Pil Yoon[a,*], Jonghee Han[a], Suk Woo Nam[a], Tae-Hoon Lim[a],
In-Hwan Oh[a], Seong-Ahn Hong[a], Young-Sung Yoo[b], Hee Chun Lim[b]

[a]*Fuel Cell Research Center, KIST, Seoul 130-650, South Korea*
[b]*Korea Electric Power Research Institute, Taejeon 305-380, South Korea*

Abstract

Yttria-stabilized zirconia (8 mol%; YSZ) or samaria-doped ceria (Sm$_{0.2}$Ce$_{0.8}$O$_2$; SDC)-modified La$_{0.85}$Sr$_{0.15}$MnO$_3$ (LSM) composite cathodes were fabricated by formation of an YSZ or SDC film at the triple-phase boundary (TPB) of LSM/YSZ/gas. The YSZ film greatly enlarged the number of electrochemical reaction sites (ERSs) by increasing the TPB. The composite cathode was formed on thin YSZ electrolyte (about 30 μm thickness) supported on an anode and then I–V characterization and ac impedance analyses were performed at temperatures between 700 and 800 °C.

As a result of the impedance analysis on the cell at 800 °C, with humidified hydrogen as the fuel and air as the oxidant, the element R_1 around the frequency of 1000 Hz is identified as the anode polarization, R_2 around the frequency of 100 Hz is identified as the cathode polarization and R_3 below the frequency of 10 Hz is the resistance of gas phase diffusion through the anode. The maximum power densities of the cell modified by the SDC sol–gel coating were about 0.53 W/cm^2 at 750 °C and about 0.19 W/cm^2 at 650 °C. The result implied that deposition of SDC in the pore surface of the cathode increased the area of the TPB, resulting in a decrease of cathode polarization and improved cell performance. © 2002 Elsevier Science B.V. All rights reserved.

Keywords: High performance cathode; Sol–gel coating; Anode-supported SOFC; Impedance analysis; Reduced-temperature SOFCs

1. Introduction

Solid oxide fuel cells (SOFCs) are prominent candidates of power generators that convert chemical energy directly and with high efficiency, into electricity while causing little pollution. For commercialization, however, high performance and stability are needed. Recently, many efforts have been devoted to develop reduced-temperature SOFCs which can minimize problems, such as electrode sintering, interfacial diffusion between electrolyte and electrode materials, and mechanical stress due to different thermal expansion coefficients (TECs) of the cell components [1,2]. Moreover, at an operating temperature down to around 700 °C, a low-cost ferritic steel interconnector can be used. However, the low operating temperature decreases cell performance because of the low ionic conductivity of yttria-stabilized zirconia (YSZ) and the high overpotential of the electrodes. To minimize resistive loses across the electrolyte, many researchers have developed anode-supported SOFCs based on thin-film electrolytes. Finally, electrode overpotentials have remained major problem.

In general, La$_x$Sr$_{1-x}$MnO$_3$ (LSM) is the most commonly used cathode material for SOFCs [3] because of its adequate compatibility with YSZ. Under normal SOFC operating conditions, however, LSM exhibits nearly electronic conductivity and therefore, the cathode reaction is limited to the triple-phase boundary (TPB) area where the LSM cathode, YSZ electrolyte and oxygen are in contact with each other [4,5]. In order to improve the performance of the LSM cathode, increase of the TPB area near the LSM/YSZ interface or extension of the TPB to the electrode is essential.

The composite cathode composed of LSM and YSZ has been extensively studied as a means to reduce electrode polarization [5–8]. It was reported that addition of YSZ to the LSM cathode enlarged the TPB area, extending the reaction site to the electrode and significantly reducing electrode polarization [5–9]. Preparation of this composite cathode includes solid-state mixing of LSM and YSZ powders followed by high-temperature sintering above 1200 °C, in order to facilitate the adhesion of the cathode on to the YSZ electrolyte. A high processing temperature, however, is not desirable since an interfacial reaction between the LSM

* Corresponding author.
E-mail address: spyoon@kist.re.kr (S.P. Yoon).

cathode and the YSZ electrolyte would take place to form highly resistant products, such as $La_2Zr_2O_7$ which eventually reduce the cell performance.

In this study, we have developed a new method of improving cathode performance by coating thin films of YSZ or samaria-doped ceria (SDC) within the pores of the $La_{0.85}Sr_{0.15}MnO_3$ cathode by a sol–gel technique [10,11]. The sol–gel technique is suitable for film formation at relatively low temperatures so that undesirable interfacial reactions can be prevented during cathode preparation [10]. Moreover, YSZ or SDC layers deposited within the LSM cathode can provide ionic paths for oxide ions, spreading the reaction site into the electrode. The effect of sol–gel coating on cell performance was investigated by ac impedance spectroscopy and dc polarization methods.

2. Experimental

2.1. Preparation of anode support and thin electrolyte

In order to fabricate a desired anode-supported cell, NiO powder and YSZ powder (Tohso Co. Ltd., TZ-8Y) were primarily mixed and milled together at a weight ratio of 50:50. Then, 24% graphite powder as a pore-former and organic binder were mixed in the powder mixture with ethyl alcohol and the mixture was dried in an oven to form a starting material for anode substrates. The starting powder mixture was compacted and pre-sintered to prepare an anode substrate at 1400 °C for 1 h. A porous anode substrate, or fuel electrode, having a porosity of 40%, was then produced. Thereafter, YSZ was coated on to the substrate by slurry coating and sintered at 1500 °C for 2 h to make a dense electrolyte layer with a thickness of about 30 μm, as shown in Fig. 1. The anode substrate was a disk shape having a diameter of about 2.5 cm and a thickness of about 1 mm [12].

2.2. Preparation of cathodes

The green layers of cathodes with 1 cm × 1 cm area were formed on the YSZ electrolyte by slurry coating of the cathode material and drying. The slurry was prepared by mixing $La_{0.85}Sr_{0.15}MnO_3$ powders (Praxair) with methyl cellulose and water. The LSM cathode was sintered at 1100 °C for 2 h. Then the layers of YSZ or SDC were deposited within the LSM cathodes by dip coating, followed by calcination at 600 °C for 2 h. In order to increase the amount of YSZ or SDC coating within the cathodes, dip coating and calcination cycles were repeated several times.

2.3. Measurement of cathode performance and single cell performance

The configuration of a symmetric cell is shown in Fig. 2. Pt gauze supplied from Alfa (52 mesh, 0.1 mm wire) was used as a current collector. The current collectors were spring
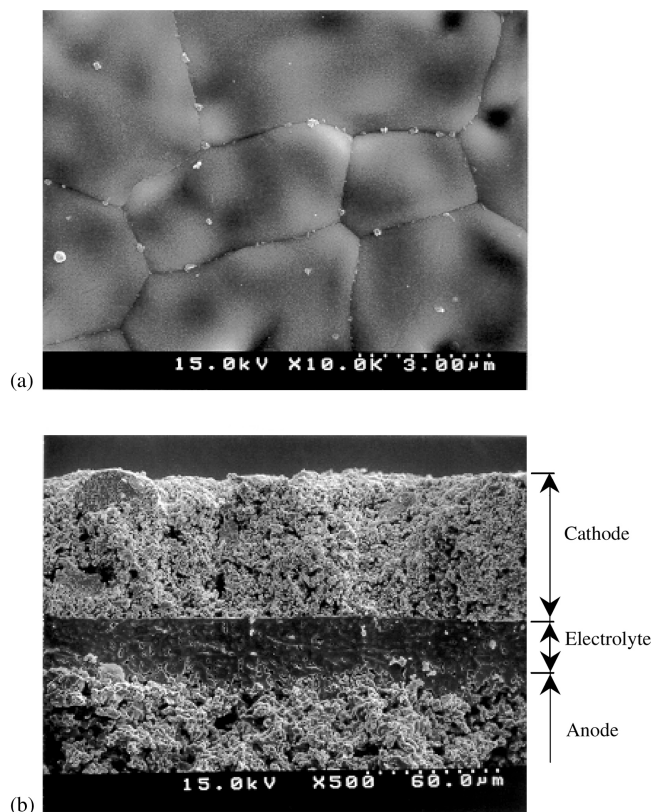

(a)

(b)

Fig. 1. SEM images of the anode-supported cell sintered at 1500 °C for 2 h: (a) surface; (b) cross-section.

loaded, as depicted in Fig. 2. In order to characterize the cathode performance, electrochemical measurements were performed with symmetric cells at the temperatures from 600 to 800 °C with N_2/O_2 or He/O_2 mixtures in the oxygen partial pressure (P_{O_2}) range of 0.01–1 atm. Gas flows were regulated with mass flow controller (Unit instruments, Inc., URS-8100) and control units (Unit instruments, Inc., URS-100-5). The gas flow rate was in the range of 50–400 cm³/min, which was enough to maintain low oxygen utilization and not to cool down the temperature of the electrodes. A Pt/(Pt + 13% Rh) thermocouple was placed near the electrodes to measure the cell temperature. The ac impedance measurements were conducted with a Solartron 1260 frequency analyzer and 1287 electrochemical interface. The ac impedance spectra in the frequency range of 0.01–10^6 Hz, with an excitation voltage of 10 mV, were taken to ensure a linear response. The I–V characterization and ac impedance analyses were also performed with the anode-supported cell modified by sol–gel coating at temperatures between 700 and 800 °C.

3. Results and discussion

3.1. Impedance analysis of symmetric cathode cells

Fig. 3 shows a typical impedance spectrum of symmetric cathode cells obtained at 800 °C under air atmosphere. Note
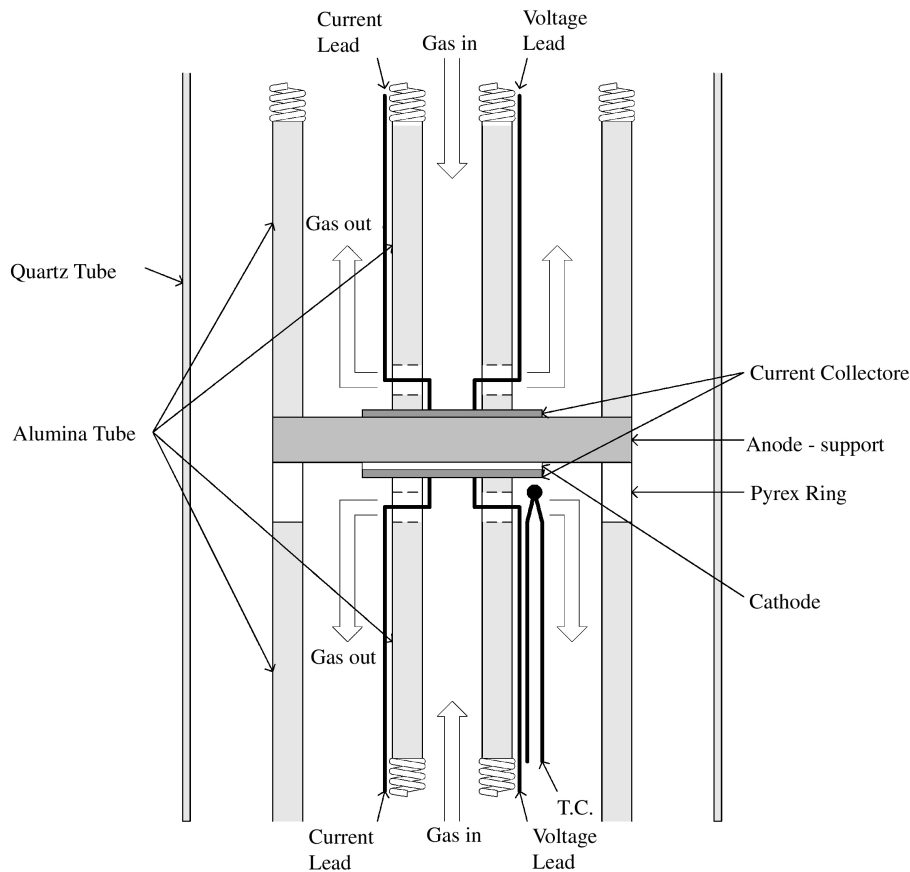
Fig. 2. Configuration of a test cell.

that the symmetric cathode cell yields an impedance spectrum including the Ohmic contribution of the electrolyte and the interface as well as the double contribution of the cathode polarization [13]. Therefore, the electrode resistance can be calculated by dividing the difference between the high and low frequency impedance intercepts by two. As can be seen in Fig. 3a, the impedance spectra decreased with increase of number of coating times. Moreover, in the case of 10 times SDC-coated LSM cathode, the electrode resistance

was only 0.08 Ω cm^2 under the same conditions (Fig. 3b). The lowest values of the electrode resistance for the various symmetric cathode cells are summarized in Table 1. The electrode resistance of the conventional cathode prepared by mixing of LSM powders and YSZ powders was about 10 Ω cm^2 at 700 °C and in an air atmosphere. On the other hand, under the same conditions, the electrode resistance of the 10 times SDC-coated cathode was only 0.19 Ω cm^2. This means that the sol–gel coating can enhance the cathode
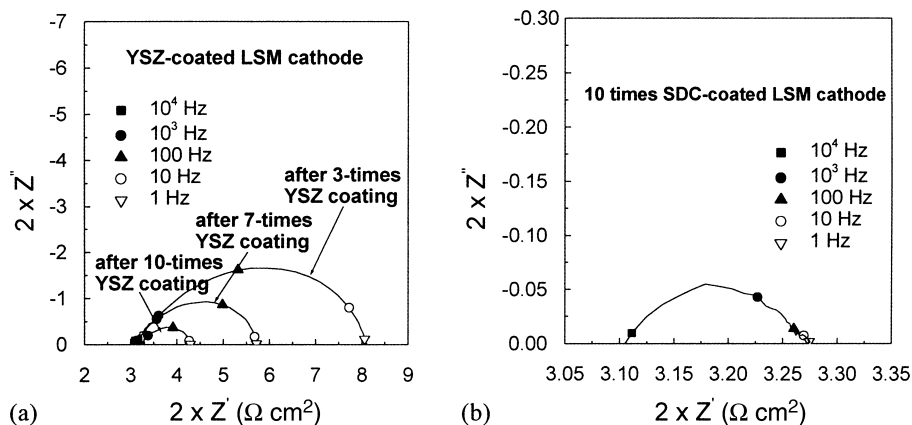

Fig. 3. Effect of sol–gel coating on the impedance spectra of symmetric cells measured at 800 °C and air atmosphere: (a) YSZ-coated LSM cathode; (b) SDC-coated LSM cathode.

Table 1
Comparison of the electrode polarization for the various cathodes

Sample	Coating time	Electrode resistance (R_{el}) (Ω cm^2)	Experimental conditions
LSM + YSZ powder	None	10	700 °C, air
YSZ-coated LSM	10	2.5	700 °C, air
SDC-coated LSM	10	0.19	700 °C, air

performance due to an increase in the number of ERSs. We have reported in our prior papers [10,11], that the enhancement of cathode performance was attributed to no formation of resistive compounds between electrode/electrolyte interface due to low processing temperature of the sol–gel coating and also resulted from an increase of the TPB due to formation of YSZ or SDC coating films. Unfortunately, however, the initial electrode resistance of the 10 times SDC-coated cathode increased with operating time, as shown in Fig. 4. But the electrode resistance of this symmetric cathode cell did stabilize at around 0.67 Ω cm^2 after operation for 500 h. The final electrode resistance was still much lower than that of the conventional cathode. Therefore, the modified cathodes were applied to the anode-supported cells and the characteristics of the single cell performance were investigated.

3.2. Impedance analysis of single cells

Fig. 5 shows impedance spectra of the anode-supported cell with 10 times YSZ-coated LSM cathode at different P_{O_2} of the cathode side while maintaining the constant P_{H_2} of the anode side. From this figure, at least four kinds of the resistance components were observed. The high frequency intercept (R_0) of the real axis (Z') exhibited no oxygen partial pressure dependence and had an activation energy of about 70 kJ/mole. Thus, R_0 represents the resistance of the bulk
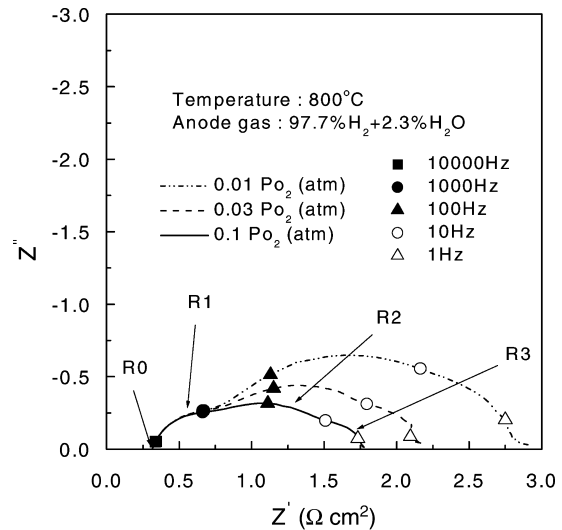
Fig. 5. Impedance spectra of the anode-supported cell with 10 times YSZ-coated cathode at different P_{O_2} of the cathode while maintaining the constant P_{H_2} of the anode.

YSZ electrolyte [14]. The value R_1, in the frequency range of around 1000 Hz was also independent of oxygen partial pressure. Therefore, the R_1 can be considered to represent the grain boundary resistance of the YSZ particles that comprise the anode support. On the other hand, the R_1 also can be thought of as the anode polarization resistance, independent of cathode polarization. As can be seen in Fig. 5, the value R_2 in the frequency range of around 100 Hz steeply increased with decrease of oxygen partial pressure. Thus, it is supposed that the R_2 stands for the cathode polarization in the single cell impedance.

In order to understand further the physical meanings of the each resistance component, the dependence of the hydrogen partial pressure was investigated with the single cell in Fig. 5. The impedance spectra of the single cell in Fig. 5, at different P_{H_2} of the anode side, while maintaining the constant P_{O_2} of the cathode side, are shown in Fig. 6. For experiments in which the water content in the fuel gas was kept constant, the hydrogen concentration was changed by mixing with nitrogen as a balancing gas while maintaining the total flow rate constant. From the Fig. 6, the R_0 and the R_2 were unchanged, while the R_1 and the R_3 were affected by the hydrogen concentration. However, the R_1 slightly decreased with decrease of hydrogen concentration, while the R_3 increased with decrease of hydrogen concentration. In addition, only the R_3 was affected as the balancing gas of N_2 was replaced with He. Therefore, the R_3 was the gas phase diffusion resistance of H_2 and H_2O, resulting from diffusion through the pores of the anode support or gas conversion by insufficient flushing.

Geyer et. al. [15] have reported that the 10 Hz relaxation is attributed to gas diffusion along the gas supply channels in their symmetric anode cells. In our study, the R_3 was independent of gas flow rate but no further experiments were performed to identify the exact physical meaning of the R_3.
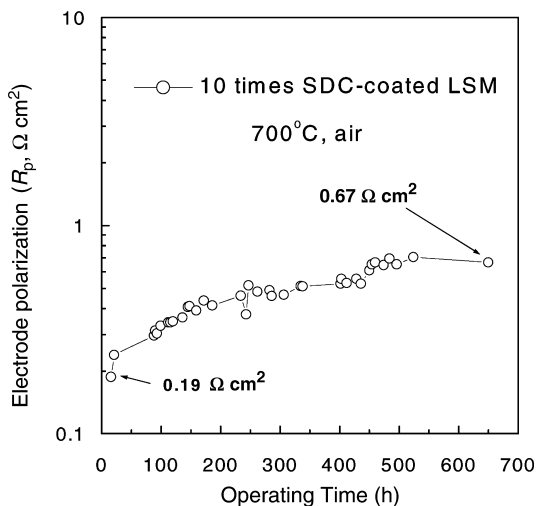

Fig. 4. Increase of electrode polarization during the test of the symmetric cathode cell with 10 times SDC-coated LSM cathode.
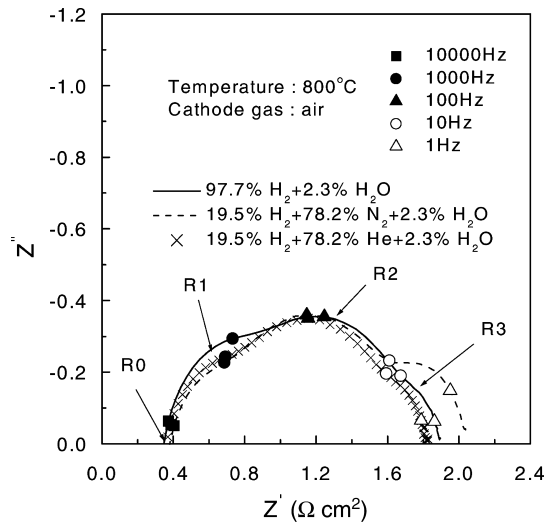
Fig. 6. Impedance spectra of the anode-supported cell with 10 times YSZ-coated cathode at different P_{H_2} of the anode while maintaining the constant P_{O_2} of the cathode.
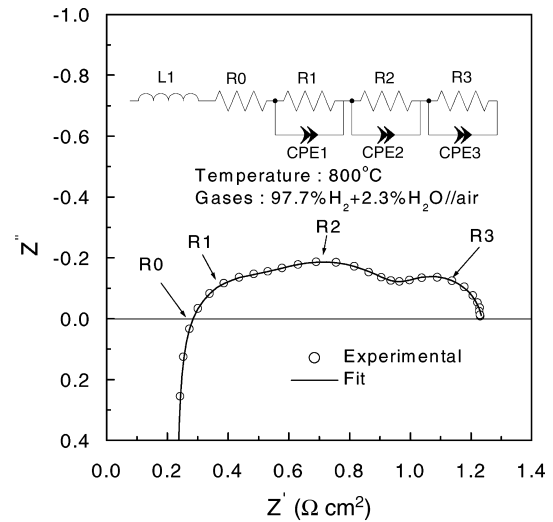

Fig. 7. Impedance spectrum obtained at 800 °C on the anode-supported cell with 10 times YSZ-coated cathode. Circles: experimental points; full line: deconvolution results including setup inductance.

Since the R_2 was affected by oxygen partial pressure at the cathode side and not affected by hydrogen partial pressure at the anode side, it is certain that the R_2 represents the cathode polarization, as mentioned above. In Fig. 6, it is of interest that the value of R_1 slightly decreased with decrease of hydrogen concentration. Assuming that R_1 is the grain boundary resistance of YSZ particles in the anode support, it should not depend on the hydrogen concentration of the anode side because the concentration and mobility of oxygen vacancy in YSZ are almost constant in these experimental conditions [16]. Recently, Jiang and Badwal [17] have studied H_2 oxidation on a Ni electrode at different H_2/H_2O ratios. They have reported that the electrocatalytic activity of Ni for H_2 oxidation significantly increases with the partial pressure of oxygen and only at constant partial pressure of oxygen increases with the partial pressure of H_2. Therefore, the anode polarization depends on the P_{H_2}/P_{H_2O} ratio as well as the H_2O content. Their results are in good agreement with the observations reported in this paper. Consequently, R_1 represents the anode polarization in the single cell impedance. To investigate the temperature dependence of each resistance component, the data from the impedance measurements in Figs. 5 and 6 were analyzed by means of an equivalent circuit which consists of an inductance (L), resistance (R) and constant phase element (CPE), as shown in Fig. 7. This overall circuit was analyzed by a complex non-linear least square (CNLS) fitting program

[18]. The activation energies of the each resistance component are summarized in Table 2. In comparison with the activation energy of the symmetric cells and the single cells, R_0 is the YSZ electrolyte resistance, R_1 the anode polarization resistance, R_2 the cathode polarization resistance and R_3 the gas phase diffusion resistance. Fig. 8 shows the impedance spectra of the single cells modified by YSZ and SDC sols. In this figure, a large decrease of R_2 for the single cell with the SDC-coated cathode was observed due to an enhancement of cathode performance.

3.3. Performance of single cells

We applied the modified LSM cathode to an anode-supported cell. Fig. 9 shows the I–V characteristics of the various single cells measured at 700 °C with humidified hydrogen as the fuel and air as the oxidant. The single cell with a non-modified LSM cathode shows poor cell performance. On the other hand, the maximum power density of the single cell with the 10 times YSZ-coated LSM cathode was about 0.2 W/cm² at the same conditions. The increase of the single cell performance was attributed to the cathode modification. The single cell with the SDC-coated cathode showed a higher power density, which resulted from higher oxygen ion conductivity of the SDC. Fig. 10 shows the performance of the single cell with the 10 times SDC-coated cathode at various temperatures. The maximum power

Table 2
Summary of activation energy values

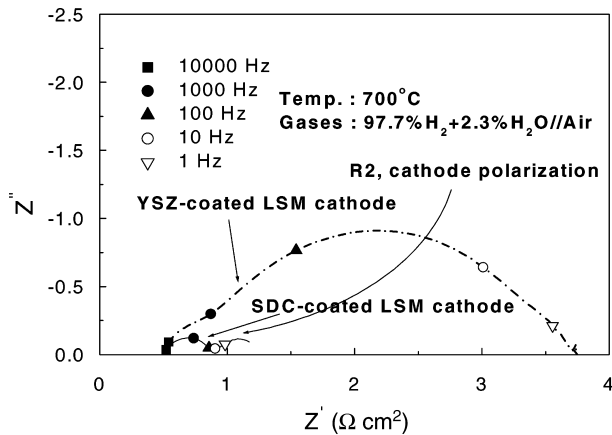| Sample	Electrode	R_0 (kJ/mole)	R_1 (kJ/mole)	R_2 (kJ/mole)	R_3 (kJ/mole)
Symmetric cell	Cathode	70 ± 5	–	140	–
	Anode		94	–	–
Single cell	–	64	82	131	$\cong 0$

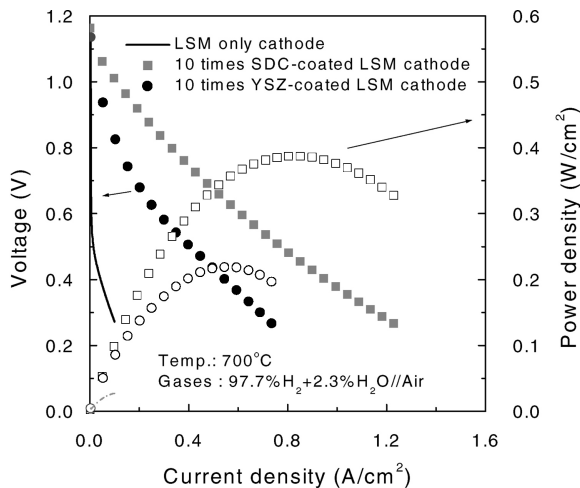Fig. 8. The impedance spectra of the single cells with modified by YSZ and SDC sols.

Fig. 9. The I–V characteristics of the various single cells measure at 700 °C with humidified hydrogen as the fuel and air as the oxidant.
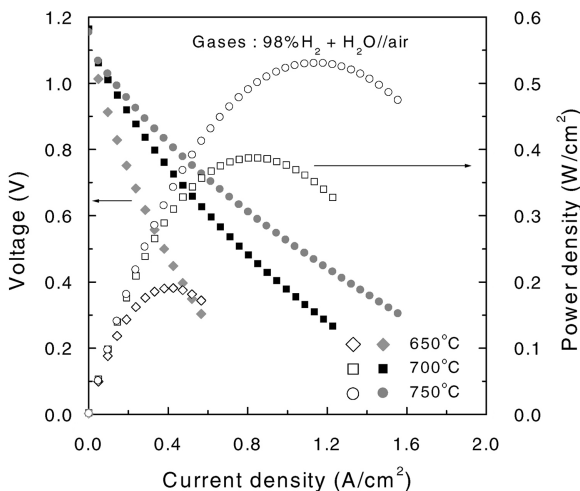

Fig. 10. The performance of the single cell with the 10 times SDC-coated cathode at various temperatures.

densities of the cell modified by the SDC sol–gel coating were about 0.53 W/cm^2 at 750 °C and about 0.19 W/cm^2 at 650 °C.

4. Conclusions

We demonstrated that sol–gel coating of YSZ or SDC within the pores of an LSM cathode increased the cathode performance. The anode-supported cells with the modified cathodes were investigated by ac impedance spectroscopy and dc polarization methods at temperatures between 700 and 800 °C. The results are as follows:

1. As results of the impedance analysis on the cell at 800 °C, with humidified hydrogen as the fuel and air as the oxidant, R_1 around the frequency of 1000 Hz represents the anode polarization, R_2 around the frequency of 100 Hz indicates the cathode polarization and R_3 below the frequency of 10 Hz was the resistance of gas phase diffusion through the anode.
2. The maximum power densities of the cell modified by the SDC sol–gel coating were about 0.53 W/cm^2 at 750 °C and about 0.19 W/cm^2 at 650 °C, with humidified hydrogen as the fuel and air as the oxidant.
3. Deposition of YSZ or SDC film in the pore surface of the cathode increased the area of TPB, resulting in a decrease of cathode polarization and increase of cell performance.

References

[1] T. Tsai, S.A. Barnett, J. Electrochem. Soc. 142 (1995) 3084.
[2] S. de Souza, S.J. Visco, L.C. De Jonghe, J. Electrochem. Soc. 144 (1997) L35.
[3] N.Q. Minh, T. Takahashi, Science and Technology of Ceramic Fuel Cells, Elsevier, Amsterdam, 1995, p. 117.
[4] M.J.L. Ostergard, C. Clausen, C. Bagger, M. Mogensen, Electrochim. Acta 40 (1995) 1971.
[5] B.C.H. Steel, Solid State Ionics 86–88 (1996) 1223.
[6] T. Kenjo, M. Nishiya, Solid State Ionics 57 (1992) 295.
[7] K. Sasaki, J.-P. Wurth, R. Gschwend, M. Godickemeier, L.J. Gauckler, J. Electrochem. Soc. 143 (1996) 530.
[8] S. Wang, Y. Jiang, Y. Zhang, J. Yan, W. Li, J. Electrochem. Soc. 145 (1998) 1932.
[9] M. Suzuki, H. Sasaki, S. Otoshi, A. Kajimura, N. Sugiura, M. Ippommatsu, J. Electrochem. Soc. 141 (1994) 1928.
[10] S.P. Yoon, S.W. Nam, T.-H. Lim, I.-H. Oh, H.Y. Ha, S.-A. Hong, Enhancement of the cathode performance by sol–gel coating of

yttria-stabilized zirconia, in: Proceedings of the Fuel Cell Seminar, Portland, OR, 2000, p. 611.

[11] S.P. Yoon, S.W. Nam, T.-H. Lim, J. Han, S.-A. Hong, Improved performance of $La_{0.85}Sr_{0.15}MnO_3$ cathode by sol–gel coatings, in: Proceedings of the Solid Oxide Fuel Cells VII, Tsukuba, Ibaraki, 2001, p. 485.

[12] Y.-S. Yoo, J.-H. Koh, J.-W. Park, H.C. Lim, Y.-H. Han, T.-K. Kang, Effect of additives on electronic performance of anode-supported solid oxide fuel cell, in: Proceedings of the Fuel Cell Seminar, Portland, OR, 2000, p. 562.

[13] S. Primdahl, M. Mogensen, J. Electrochem. Soc. 145 (1998) 2431.

[14] J.E. Bauerle, J. Phys. Chem. Solids 30 (1969) 2657.

[15] J. Geyer, H. Kohlmuller, H. Landes, R. Stubner, Investigation into kinetics of the Ni–YSZ cermet-anode of a solid oxide fuel cell, in: Proceedings of the Solid Oxide Fuel Cells V, Aachen, 1997, p. 585.

[16] N.Q. Minh, T. Takahashi, Science and Technology of Ceramic Fuel Cells, Elsevier, Amsterdam, 1995, p. 69.

[17] P. Jiang, S.P.S. Badwal, J. Electrochem. Soc. 144 (1997) 3777.

[18] ZView version 2.1b, Scribner Associates Inc.